materials proceedings

MDPI

Proceeding Paper

Biosynthesis of Titanium Dioxide Nanoparticles by the Aqueous Extract of *Juglans regia* Green Husk †

Zahra Heydari and Parinaz Ghadam *

Department of Biotechnology, Faculty of Biological Sciences, Alzahra University, Tehran 1993893973, Iran;
* Correspondence: pghadam@alzahra.ac.ir
† Presented at the 4th International Online Conference on Nanomaterials, 5–19 May 2023; Available online: https://iocn2023.sciforum.net.

Abstract: A straightforward, non-toxic, economical, and environmentally safety method for nanoparticles (NPs) synthesis is NPs biosynthesis. An aqueous extract of the green husk of *Juglans regia* (*J. regia*) was used to produce titanium dioxide NPs (TiO_2 NPs) in this study. The green husk of walnuts is an agricultural waste that may contain valuable compounds. Numerous studies have demonstrated the potential of this inexpensive natural material as a source of phenolic compounds with antiradical and antimicrobial properties. The NPs were characterized using UV-Vis spectroscopy, X-ray diffraction, FT–IR spectrum, DLS, and FE-SEM. At 334 nm, the UV–visible spectrum had a significant peak. The TiO_2 NPs that were made had two distinct phases that ranged in size from 19 to 23 nm on average. FT-IR analysis revealed the Ti-O bond. FE-SEM and EDX were used to characterize the spherical surface morphology and their Ti and O elemental configurations, respectively. TiO_2NPs are viewed as incredibly important nanomaterials as a result of their security, high strength and photocatalytic exercises. Accordingly, TiO_2 NPs are valuable in beauty care products, substance detecting, wastewater treatment, antimicrobial applications, hydrogen creation and lithium-particle batteries.

Keywords: biosynthesis; green synthesis; Titanium dioxide; *Juglans regia* green husk; Anatase

1. Introduction

Nontechnology is a developing part of the science and innovation which is hugely creating. The creation or synthesis of nanomaterials, known as nanomaterials, is the science behind nanotechnology [1]. Organic and inorganic materials are the two types of nanomaterials that fall within the range of 1–100 nm [2,3]. Methods that are biological, physical, and chemical are used to create nanomaterials. The bio-based protocols for synthesis of NPs are green synthesis, simple, inexpensive, and suitable for larger-scale production [2,4]. The synthesis of NPs using biological agents has received a lot of attention in the nanotechnology over these decades [4].

TiO_2 NP is regarded as one of the most valuable NPs because it is non-toxic, chemically and thermally stable, inexpensive, and photo catalytically active [5,6]. There are three distinct polymorphs of binary metal oxides, each of which has a crystalline structure: brookite, rutile, and anatase. Rutile TiO_2 has a bandgap energy of 3.0 eV, anatase TiO_2 has a bandgap energy of 3.2 eV, and brookite TiO_2 has a bandgap energy of 3.2 eV. Self-cleaning solar cells, chemical sensing, gas sensors, anti-fogging, antimicrobial, deodorization, waste water treatment, cosmetics applications, hydrogen production, and lithium-ion batteries are just a few of the many fields in which TiO_2 has received significant attention in recent decades [1,5,6]. Photocatalysis is thought to be the most useful of these because it uses sunlight to break down organic pollutants [5]. We have reported TiO_2 biosynthesis using an aqueous solution of the *J. regia* green husk in this study.

Citation: Heydari, Z.; Ghadam, P. Biosynthesis of Titanium Dioxide Nanoparticles by the Aqueous Extract of *Juglans regia* Green Husk. *Mater. Proc.* **2023**, *14*, x. https://doi.org/10.3390/xxxxx

Academic Editor(s):

Published: date

2. Materials and Methods

2.1. Materials

Titanium tetra isopropoxide-Analytical MERCK KGaA in Germany supplied the titanium tetraisopropoxide (TTIP, $Ti(OC_3H_7)_4$, purity ≥ 98 percent). The green husk was taken from Iran's Zanjan. During the process of making leaf extract, distilled water and filter papers from Whatman, England, with pores measuring 1.2 m were used. The NPs were synthesized using deionized water as the solvent, and no other reagents were altered in any way.

2.2. Synthesis Method

Preparation of *J. regia* Green Husk Powder

Subsequent to drying of *J. regia* green husk, 0.4 g of the powder were broken up 15 mL of refined water and warmed at 100 °C involving bain-marie for 10 min. The extract was made after filtering the yellowish solution with filter papers.

2.3. TiO_2NPs Production

The sum 50 μL of TTIP arrangement was blended in with 0.5 mL plant remove and 4.5 mL twofold refined water was added to orchestrate the G-TiO_2NPs. The consolidated arrangement was blended for 24 h. at surrounding temperature. The yellowish encourage was shaped and the variety development was proof of the NP arrangement. The arrangement was centrifuged at 5304× *g* for 10 min, and washing were rehashed for multiple times. Gotten NP was grounded and considered calcinations at 600 °C in a stifle heater for 4 h [6]. The determined TiO_2NPs were put away for scientific portrayal.

2.4. Characterization of TiO_2NPs

UV-visible spectra were obtained with a Shimadzu UV-1800 spectrophotometer (Shimadzu Company, Kyoto, Japan) with a frequency scope of 200–800 nm. The sort and state of translucent were examined by X-beam diffraction investigation utilizing Rigaku Ultima IV (Japan). The useful gatherings and metal holding were broken down by FT-IR spectroscopy in the conveyance mode in the scope of 4000–400 cm^{-1} by BRUKER (TENSON 27, Germany). The hydrodynamic still up in the air with a CORDOUAN Innovation (VASCO TM, France). The morphology, the size of NPs and leaving components were examined by FESEM and EDX utilizing TESCAN (MIRA3, Czechia). An electric stifle heater was utilized for calcination of TiO_2NPs (Azar Heaters organization, Iran).

3. Results and Discussion

3.1. UV—Vis Analysis

The Surface Plasmon Resonance (SPR) of TiO_2NPs revealed a maximum absorbance in the 300–350 nm range, indicating that colloidal titanium and titanium ions had exchanged (Figure 1) [7].

The equation 1 was used to calculate the TiO_2NPs' energy band gap.

$$Eg = hc/\lambda \quad (1)$$

where h is the constant of Planck (4.135×10^{-15} eV·s); c is the wavelength (in nm) and the speed of light (3×10^{8} ms^{-1}) [8]. The absorption peak is located at a wavelength of 338 nm, where the band gap was calculated to be 3.67 eV.

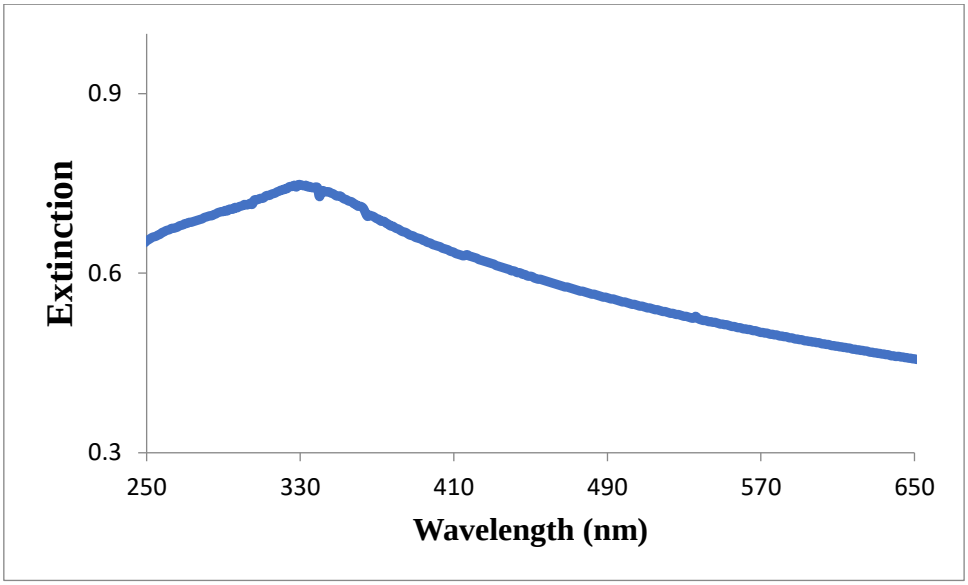

Figure 1. UV-Vis spectrum of synthesized TiO_2NPs.

3.2. XRD Analysis

The X-ray diffraction (XRD) method broke down the translucent stage, gem construction, and virtue of the NP. Figure 2 depicts the TiO_2NPs' XRD pattern. It also confirms that biosynthesized TiO_2NPs are crystalline. The XRD pattern correctly depicts eight strong, broad peaks across the entire range of 2 values. Figure 2 showcases conspicuous diffraction tops at 25.29°, 37.98°, 47.98°, 53.99°, 55.02°, 62.65°, 70.43° and 73.3° ordered as (101), (004), (200), (211), (211), (002), (220) and (215) mill operator records esteem separately. In the meantime, the sample's XRD patterns reveal a mix of anatase and rutile. The major plane of anatase is observed to be the plane (101) while the major plane of rutile is observed to be the plane (211). Anatase and rutile are mixed in the sample. The major plane of anatase was found to be the (101) plane, and the major plane of rutile was found to be the (110) plane. The ICDD file No. is consistent with these findings. Anatase is 01-083-2243, and rutile is 00-004-0551 [9]. The major peak at 25.29 in the synthesized NPs' XRD pattern corresponds to the TiO_2 anatase (101) crystallographic plane. Using Debye–Scherrer's Equation (2), TiO_2 NPs average crystallite size was determined from the XRD pattern [10]:

$$D = K\,\lambda/(\beta \cos \theta) \quad (2)$$

D where; K is the crystal's size; the wavelength of x-ray radiation is 0.15418 nm at constant Scherrer (K = 0.89); the full width at half maximum (FWHM) of the diffraction peak in relation to the crystallographic plane of anatase and the angle of the x-ray diffraction peak. The estimated and calculated sizes of the crystallites are presented in Table 1. In addition, a crystallite's average size of 11.45 nm was discovered.

Table 1. The structural and geometrical parameters of TiO_2NPs.

Sr No.	Peak Position 2θ (Degree)	FWHM Left [9]	Lattice Planes (h k l)	Inter-Planar Distance d Spacing (nm)	Crystallite Size D (nm)
1	25.295	0.56	101	3.51812	14.44
2	37.98	0.85	004	2.36692	9.82
3	47.98	0.76	200	1.89456	11.36
4	53.99	0.52	211	1.69713	17.13
5	55.02	0.6	211	1.66753	15.42

6	62.65	2.0	002	1.48155	4.62
7	70.43	0.7	220	1.33585	13.88
8	75.3	2	215	1.26074	4.98

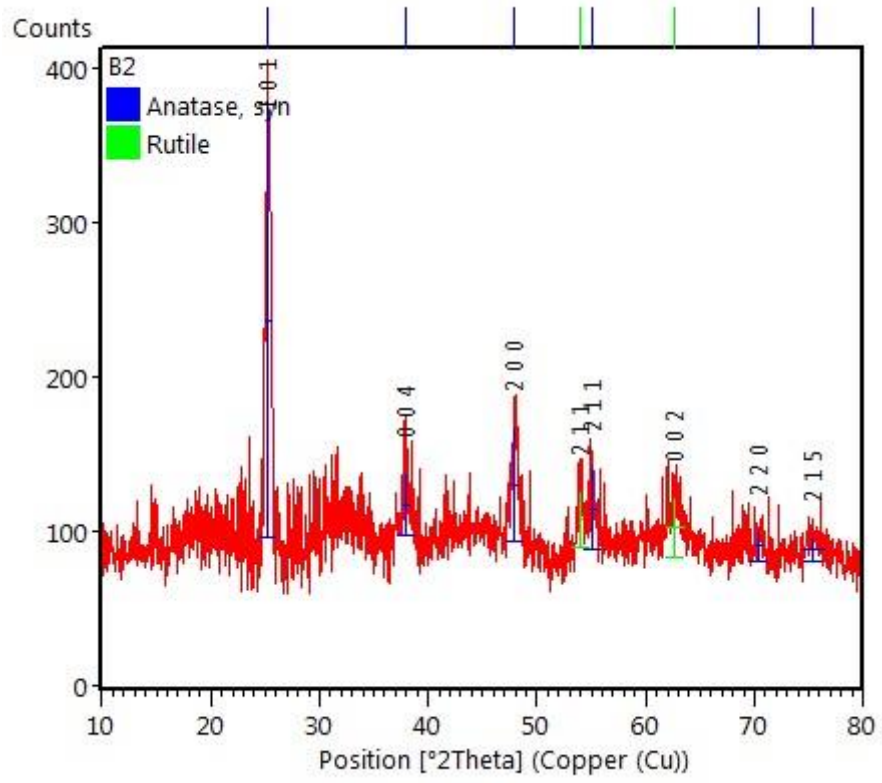

Figure 2. XRD patterns of TiO_2NPs.

3.3. Fourier Transforms Infrared (FT-IR) Spectroscopy

The utilitarian gatherings and substance compound decide utilizing the FT-IR range. The TiO_2NPs FT–IR plot is depicted in Figure 3. The O–H Stretching vibration is correlated with the broadband at 3709–3712 cm^{-1}. The bending vibration of functional groups C–H is reflected in the band between 1513 and 1516 cm^{-1} [2]. Below 1200 cm^{-1}, the characteristic absorption band of green-synthesized TiO_2NPs was observed. The Ti-O-Ti vibrations are primarily responsible for this distinctive absorption peak [1]. The –OH stretching was the cause of the peak around 3000 cm^{-1} [8]. The spectrum shows peaks at 1365 cm^{-1} for nitro compounds, 1544 cm^{-1} for amide-II from proteins, 1642 cm^{-1} for H-O-H bending vibrations, and 1796–1725 cm^{-1} for carbonyl (polyol) esters [11]. Table 2 displays the tentative frequency and the band assignment. These parts have various natural useful gatherings which append on the outer layer of TTIP and cause the decrease of TTIP. As a result, they serve as both capping agents and reducing agents.

Table 2. FT-IR analysis of TiO_2NPs.

S.NO	Wave Number (cm^{-1})	Band Assignment
1	3709–3712 cm^{-1}	O–H stretching vibration
2	3000 cm^{-1}	–OH stretching
3	1796–1725 cm^{-1}	carbonyl (polyol' s) esters
4	1642 cm^{-1}	H–O–H bending vibrations
6	1544 cm^{-1}	amide-II from proteins

7	1513–1516 cm^{-1}	Bending vibration of functional groups C–H
8	1365 cm^{-1}	nitro compounds
9	below 1200 cm^{-1}	Ti–O and Ti–O–Ti bending vibrations

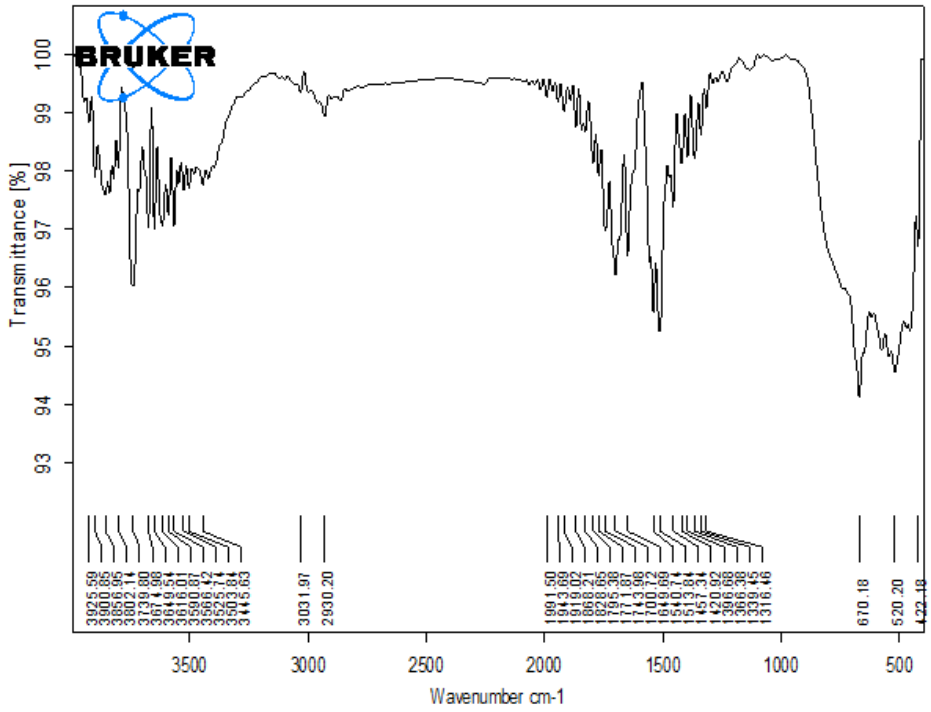

Figure 3. FT–IR spectra of TiO_2NPs.

3.4. Dynamic Light Scattering (DLS) Analysis

The hydrodynamic diameter of biosynthesized TiO_2NPs was exactly measured using particle size analysis. The mean particle size of biosynthesized TiO_2NPs was estimated to be 129.68. Figure 4 showed the particle size distribution curve for biosynthesized TiO_2.

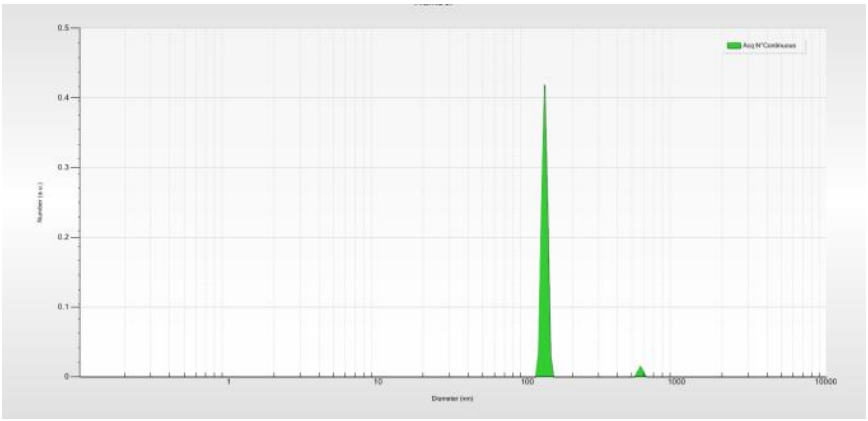

Figure 4. DLS analysis.

3.5. Field Emission Scanning Electron Microscopy (FE-SEM) Images

The surface morphology and histogram of the NPs are introduced in Figure 5. The spherical shape of TiO_2NPs was seen in three-dimensional images (Figure 5a, which was evident from the enlarged images (at 4 K, 10 K, 15 K, and 50 K, respectively)). It has been suggested that the excess H^+ ions of H_2O molecules on the surface of TiO_2NPs could be the cause of aggregation. Through van der Waals forces, these ions reduce the repulsion

between TiO_2 and TiO_2 molecules [11]. EDAX analysis was used to conduct a compositional analysis of the synthesized TiO_2NPs. As depicted in Figure 5b contained 61.51 percent weight of Ti, 34.89 percent oxygen, 2.73 percent potassium, and 0.87 percent carbon. The presence of TiO_2 NPs is confirmed by this. The presence of biomolecules in the extract of *J. regia* green husk is the cause of the observed C and K peaks [12]. The histogram of the TiO_2NPs' distribution of particle sizes is shown in Figure 5c.

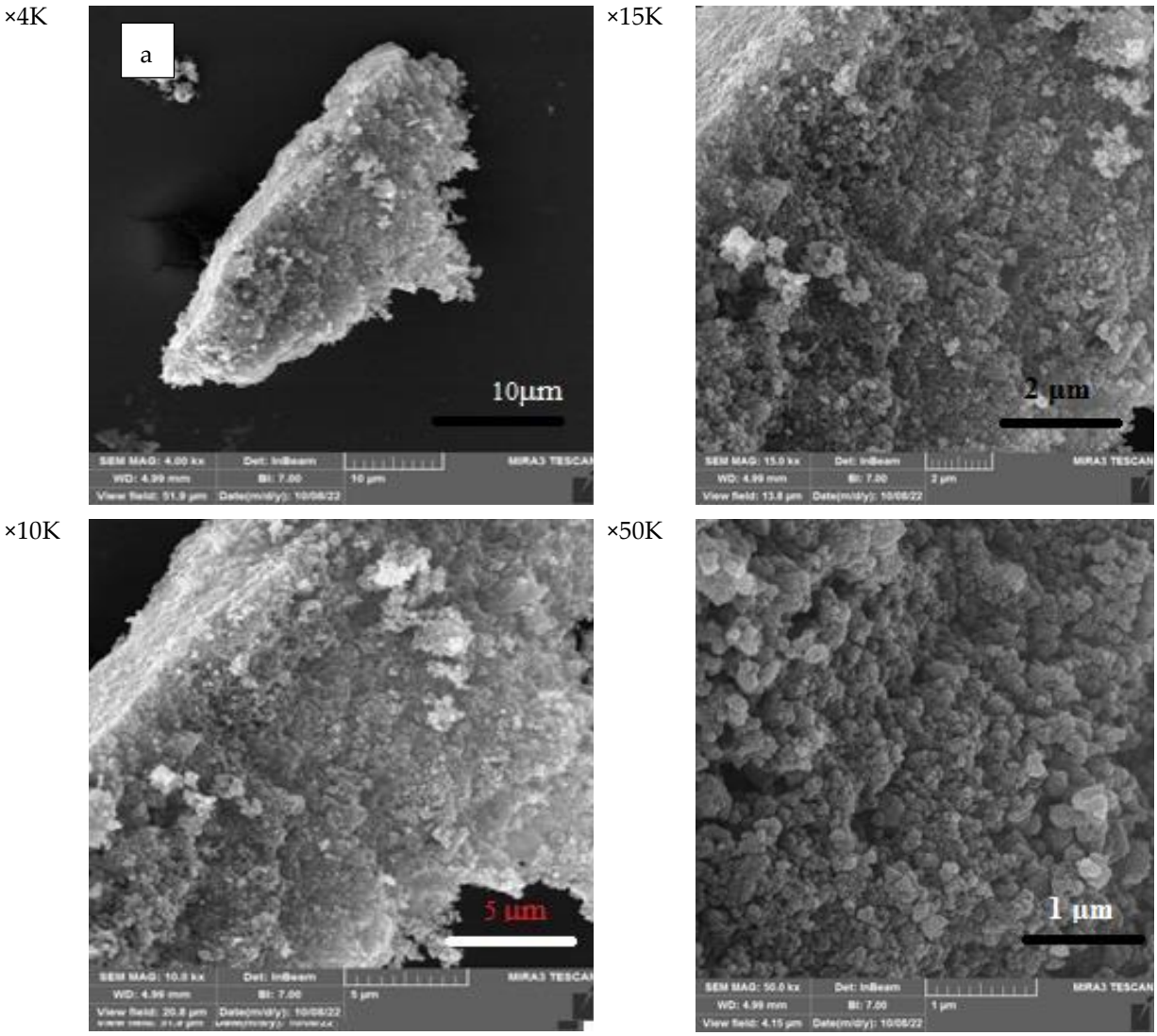

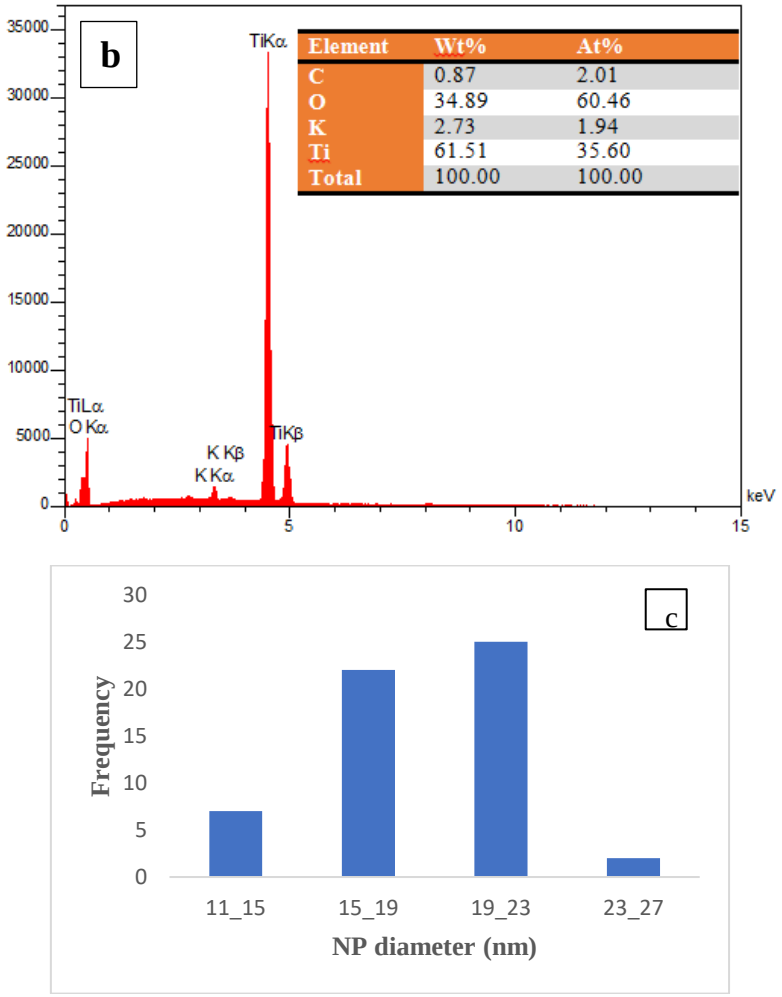

Figure 5. (**a**) FE-SEM (**b**) EDX image of synthesized TiO_2NPs and (**c**) Histogram of TiO_2NPs size distribution.

4. Conclusions

The synthesis of TiO_2NPs using *J. regia* green husk aqueous extract successfully synthesized using the biosynthesis method. UV–Vis Spectroscopy, XRD, FT-IR, DLS, and FE-SEM were used to examine the optical and structural properties of synthesized NPs. The XRD, DLS, and SEM results revealed that the two distinct polymorphs of TiO_2NPs had spherical morphology and an average diameter of 19–23 nm. The calculated energy band gap of the synthesized TiO_2NPs was 3.67 eV, which was greater than the band gap of bulk TiO_2 (3.2 eV). The role of leaf extract in TiO_2NP synthesis is determined by FT-IR analysis. The current study demonstrates that the novel biosynthesis of TiO_2NPs made possible by the use of *J. regia* aqueous extract of the green husk is a method that makes use of inexpensive precursors. This easy, cost-effective, and green synthesis method is used in a variety of applications.

References

1. Ahmad, W.; Jaiswal, K.K.; Soni, S. Green synthesis of titanium dioxide (TiO_2) nanoparticles by using Mentha arvensis leaves extract and its antimicrobial properties. *Inorg. Nano-Met. Chem.* **2020**, *50*, 1032–1038.
2. Aravind, M.; Amalanathan, M.; Mary, M.S.M. Synthesis of TiO_2 nanoparticles by chemical and green synthesis methods and their multifaceted properties. *SN Appl. Sci.* **2021**, *3*, 409.
3. Patidar, V.; Jain, P. Green synthesis of TiO_2 nanoparticle using Moringa oleifera leaf extract. *Int. Res. J. Eng. Technol.* **2017**, *4*, 1–4.

4. Keat, C.L.; Aziz, A.; Eid, A.M.; Elmarzugi, N.A. Biosynthesis of nanoparticles and silver nanoparticles. *Bioresour. Bioprocess.* **2015**, *2*, 47.
5. Muniandy, S.S.; Kaus, N.H.M.; Jiang, Z.-T.; Altarawneh, M.; Lee, H.L. Green synthesis of mesoporous anatase TiO_2 nanoparticles and their photocatalytic activities. *RSC Adv.* **2017**, *7*, 48083–48094.
6. Ahn, E.-Y.; Shin, S.-W.; Kim, K.; Park, Y. Facile green synthesis of titanium dioxide nanoparticles by upcycling mangosteen (Garcinia mangostana) pericarp extract. *Nanoscale Res. Lett.* **2022**, *17*, 40.
7. Hunagund, S.M.; Desai, V.R.; Barretto, D.A.; Pujar, M.S.; Kadadevarmath, J.S.; Vootla, S.; Sidarai, A.H. Photocatalysis effect of a novel green synthesis gadolinium doped titanium dioxide nanoparticles on their biological activities. *J. Photochem. Photobiol. A Chem.* **2017**, *346*, 159–167.
8. Mathew, S.S.; Sunny, N.E.; Shanmugam, V. Green synthesis of anatase titanium dioxide nanoparticles using Cuminum cyminum seed extract; effect on Mung bean (Vigna radiata) seed germination. *Inorg. Chem. Commun.* **2021**, *126*, 108485.
9. Gupta, K.; Singh, R.; Pandey, A.; Pandey, A. Correction: Photocatalytic antibacterial performance of TiO_2 and Ag-doped TiO_2 against S. aureus. P. aeruginosa and *E. coli*. *Beilstein J. Nanotechnol.* **2020**, *11*, 547–549.
10. Jenkins, R.; Snyder, R.L. *Introduction to X-ray Powder Diffractometry (Volume 138)*; Wiley Online Library: Hoboken, NJ, USA, 1996.
11. Kaur, H.; Kaur, S.; Singh, J.; Rawat, M.; Kumar, S. Expanding horizon: Green synthesis of TiO_2 nanoparticles using Carica papaya leaves for photocatalysis application. *Mater. Res. Express* **2019**, *6*, 095034.
12. Abbasi, Z.; Feizi, S.; Taghipour, E.; Ghadam, P. Green synthesis of silver nanoparticles using aqueous extract of dried Juglans regia green husk and examination of its biological properties. *Green Process. Synth.* **2017**, *6*, 477–485.